

# Experimental studies of nonlinear laser-plasma interactions and hot electrons\*

Qi Lan-Ying(祁兰英), Zheng Zhi-Jian(郑志坚), Mei Qi-Yong(梅启庸), Li San-Wei(李三伟),  
Zhao Xue-Wei(赵雪薇), Xie Ping(谢平), Li Wen-Hong(李文洪),  
Yang Xiang-Dong(杨向东), Tang Dao-Yuan(唐道源), and Ding Yao-Nan(丁耀南)  
(*Institute of Nuclear Physics and Chemistry, China Academy of Engineering Physics, Chengdu 610003*)

**Abstract** Observation shows that the stimulated Raman scattering (SRS) in a cavity target irradiated by  $1.053\mu\text{m}$  laser is the dominant mechanism in producing hot electrons. In cavity targets, stimulated Brillouin scattering (SBS) and SRS are main abnormal absorption processes, they can scatter about 0.4 of the laser light energy fraction.

**Keywords** Cavity target, Nonlinear interaction, Hot electron, Stimulated Raman scattering, Stimulated Brillouin scattering

## 1 Introduction

All nonlinear processes are intensively related to parameters of laser light and characteristics of the plasmas. SRS(stimulated Raman scattering) and SBS(stimulated Brillouin scattering) are harmful to plasma stabilities because of their potentialities to decrease the amount of energy delivered to the target and increase the generation of fast electrons and hard X-rays. They can play a significant destructive role in X-rays driven implosion, as they can develop in the long scalelength plasma that expands and fills up the cavity.

## 2 Experimental

The experiments were performed<sup>[1,2]</sup> on the Shanghai "Shenguang-I" Nd: glass laser facility. The laser parameters were as follows: output energy  $E_L = 50 \sim 700\text{ J}$  for  $\lambda = 1.053\mu\text{m}$ ,  $E_L = 100 \sim 200\text{ J}$  for  $\lambda = 0.53\mu\text{m}$ , laser intensity  $I_L = 5 \times 10^{13} \sim 5 \times 10^{15}\text{ W/cm}^2$ . We categorized our experimental targets into two types: gold disk targets, gold cavity ones.

In the experiments the quantities we have measured include back-scattered SRS, SBS light energy measured by two laser energymeters; the angular distribution of SRS energy measured by the new polyvinylidene fluoride thermoelectric detectors; the time-integrated spectra of SRS, SBS;  $2\omega_0$ ,  $(3/2)\omega_0$  lights measured by using an

optical multiple-channel analyser with  $(1/4)\text{ m}$  grating.

An absolutely-calibrated hard X-ray spectrometer of  $1.5 \sim 300\text{ keV}$  is composed of a ten-channel filter-fluorescer system (F·F) and a five-channel K-edge filter system (K·F)<sup>[3]</sup>. The hot electrons temperature  $T_h$  and superhot electrons temperature  $T_{hh}$  are commonly derived from the slope of hard X-ray spectrum. The angular distribution of the hard X-rays ( $10 \sim 150\text{ keV}$ ) has also been detected by a GaAs photoelectric detector array.

## 3 Results and discussions

3.1 Time-integrated spectra of nonlinear processes for a cavity target at  $\lambda = 1.053\mu\text{m}$ .

A) Spectra of harmonic and up-scattered SRS lights (see Fig.1).

a) (530nm)  $2\omega_0$  light:  $E \approx 2 \times 10^{-3} \times E_{\omega_0}$  ( $E_{\omega_0} = 340 \sim 380\text{ J}$ )

b) (709nm)  $(3/2)\omega_0$  light:  $E \approx 6 \times 10^{-3} \times E_{\omega_0}$

c) (730~800nm) up-scattered SRS light

d) (1053nm)SBS scattering light. The fraction of SBS energy is  $0.2 \sim 0.3$  of laser energy.

B) Spectrum of back-scattering SRS light(see Fig.2). Spectrum wavelength is from  $1.2$  to  $1.9\mu\text{m}$ . Its peak wavelength is  $1.8\mu\text{m}$ , which corresponds to  $n_e \sim 0.15n_c$ . Where  $n_e$  is the electrons density,  $n_c$  is the critical

\*The Project Supported by National Natural Science Foundation of China, and the National High Technology 863 Plan 416 special subject.

Manuscript received date: 1995-10-20

electron density. The fraction of SRS energy is 0.10~0.15 of laser energy.

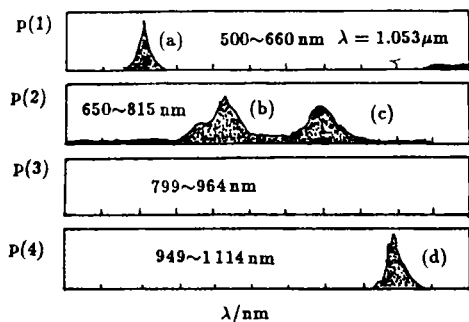


Fig.1 Time-integrated spectrum of nonlinear processes for a cavity target

3.2 Angular distribution (see Fig.3) of SRS for cavity targets irradiated by 1.053  $\mu\text{m}$  is the most intensive at the backward. The curve shape is similar to angular distribution of planar target<sup>[4]</sup>. This indicates that in cavity targets SRS occurs near the inlet hole.

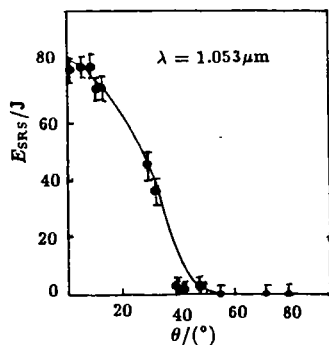


Fig.3 Angular distribution of SRS

3.3 Spectrum (see Fig.4) of hard X-rays inside the cavity has three temperatures (thermal electron temperature,  $T_e = 1.7 \sim 3.5$  keV,  $T_h = 35 \sim 50$  keV,  $T_{hh} = 130 \sim 350$  keV) which shows that two groups of high energy electrons obey Maxwellian distribution in cavity targets. Although the energy of incident laser is nearly the same for the planars as the cavity targets, the fraction of hot electrons and  $T_h$  of cavity targets both are bigger than those of planar targets (see Fig.5). Because of the cavity confinement for the plasma, the density-gradient scale-length  $L$  in the density region  $n_e < n_c/4$  for a cavity target is larger than that for a planar target, which results in increasing electron en-

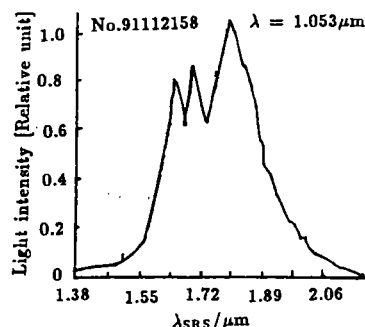


Fig.2 Spectrum of back-scattered SRS light

ergy and SRS, and hardening the corresponding X-ray spectrum.

In order to correct theoretical model and improve accuracy of calculating the total energy of hot electrons in cavity, it is urgent to identify the traveling direction of hot electrons and the regions of hard X-ray generation. In our experiment reported here we designed two kinds of specific structure gold cavities: JC-4 and JC-3<sup>[5]</sup>. There were two layers of Formvar foils in cavities. The first layer of foil is 0.3  $\mu\text{m}$  thick, and 250  $\mu\text{m}$  from the entrance, the input laser beam impinged it first. The second layer of foil was mounted at the bottom of the cavity. We called the structure of target as JC-3. The difference of target JC-4 from target JC-3 is that there is a piece of 20  $\mu\text{m}$  thick gold disk mounted closely behind the second foil. The typical experimental results of specific structure cavity targets are shown in Fig.6.  $E_{\text{HXT}}$  is total energy of hard X-rays (10~100 keV) outside cavity targets, it is corrected by the angular distribution of hard X-rays. The  $E_{\text{HXT}}$  is normalized by the  $E_{\text{SRS}}$ , i.e.  $\eta = E_{\text{HXT}}/E_{\text{SRS}}$ ,  $\eta(\text{JC-4})/\eta(\text{JC-3}) \approx 2.5$ ,  $\Delta\eta \approx 1.5$ . It is clear that the increased 1.5 times energy of hard X-rays is produced by hot electrons interaction with the additional gold disk in target JC-4. The results show that most of the hot electrons in cavity travel along the direction of laser beam, collide with cavity wall and emit hard X-rays through bremsstrahlung effect.

Theoretically, hot electrons are produced by Langmuir waves in laser-produced plasma, which are excited by incident laser wave. Res-

onance absorption (RA), Two plasmon decay(TPD), Ion acoustic decay(IAD) nonlinear processes, etc are regarded as the main mechanism to drive Langmuir wave. Many experimental results showed that under the condition of large focus dimension or large scalelength, the hot electrons are mainly produced by stimulated Raman plasma scattering<sup>[6,7]</sup>. Our experimental results of cavity targets show that total energy of hot electrons has a linear relation with

total energy of SRS light(see Fig.7),  $E_{\text{SRS}}$  is roughly equal to  $E_{\text{HE}}$  for  $E_{\text{L}} \approx 320 \sim 400\text{J}$ ,  $\tau \approx 800 \sim 900\text{ps}$ ,  $\lambda = 1.053\mu\text{m}$ . Generally, fraction of the energy is  $\sim 0.1$  of incident laser energy. The highest is up to 0.2. And  $E_{2\omega_0}$  and  $E_{(3/2)\omega_0}$  are nearly  $0.001 \sim 0.002$  and  $0.004 \sim 0.005$  of incident energy fraction, respectively. So our conclusion agrees well with those other researchers have got<sup>[8,9]</sup>.

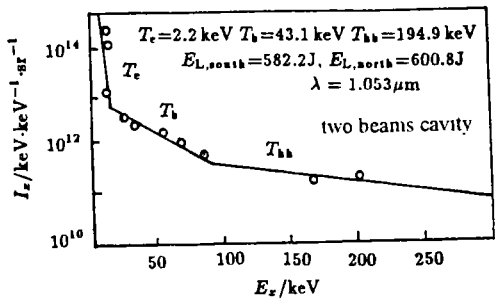


Fig.4 Spectrum of hard X-rays inside the cavity

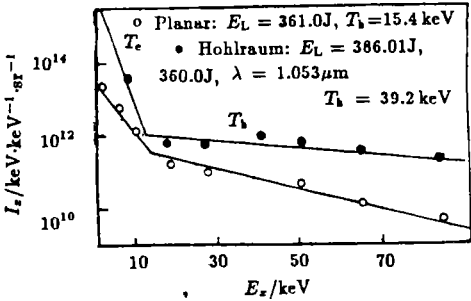


Fig.5 Comparison of spectra of hard X-rays between the planar target and cavity target

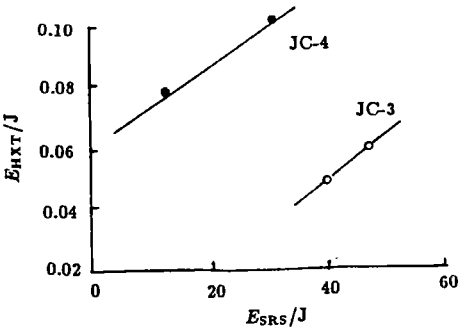


Fig.6 Experimental results of cavity targets

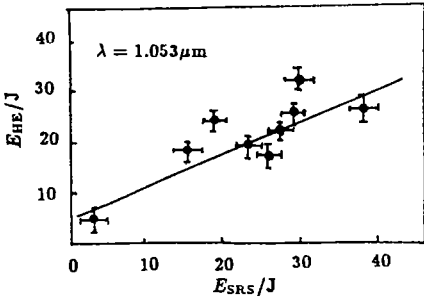


Fig.7 Correlation between  $E_{\text{SRS}}$  and  $E_{\text{HE}}$

3.4 SRS and hot electrons both have a close relation with laser parameters as well as the scale length of plasma (see Table 1, Figs.8,9).

Table 1 Hot electrons and SRS from targets irradiated with 0.53 and 1.053μm light

Targets	$\lambda/\mu\text{m}$	$E_{\text{SRS}}/E_{\text{L}}$	$E_{\text{HE}}/E_{\text{L}}$	$T_{\text{e}}/\text{keV}$	$T_{\text{h}}/\text{keV}$
Au disk target	1.053	$4 \times 10^{-3}$	$2.8 \times 10^{-2}$	3.72	13.6
	0.53	$2 \times 10^{-5}$	$3.1 \times 10^{-3}$	1.50	8.5
Cylindrical target	1.053	$1 \sim 1.5 \times 10^{-1}$	$1.8 \times 10^{-1}$	—	27~35
	0.53	$2 \times 10^{-3}$	$3.5 \times 10^{-3}$	—	15~20

Table 1 shows that the total energy of hot electrons produced by laser of 0.53μm wavelength is about one to two order of magnitude less than that of 1.053μm; fraction of SRS energy decreases about two order of magnitude,  $T_{\text{h}}$  and  $T_{\text{e}}$  reduce about one half. Shorter wavelength laser can be used to suppress SRS because of increasing electron-ion collision. At

the same conditions,  $E_{\text{SRS}}$  of cavity target ( $\phi 400\mu\text{m} \times 200\mu\text{m}$ ) and planar target ( $\phi 210\mu\text{m}$ ) are 200 times and 20 times larger than that

of planar target ( $\phi 60\mu\text{m}$ ), respectively. Fig.9 shows that SRS energy dramatically increases as the laser energy increases.

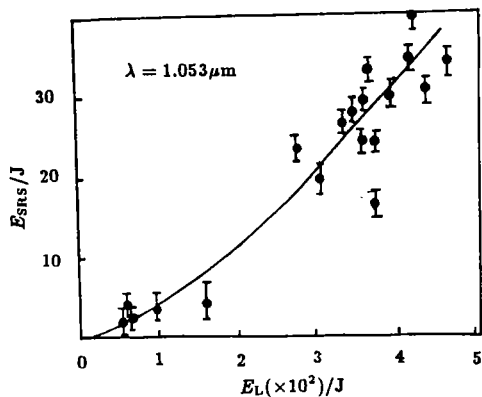


Fig.8 SRS energy vs incident laser light energy

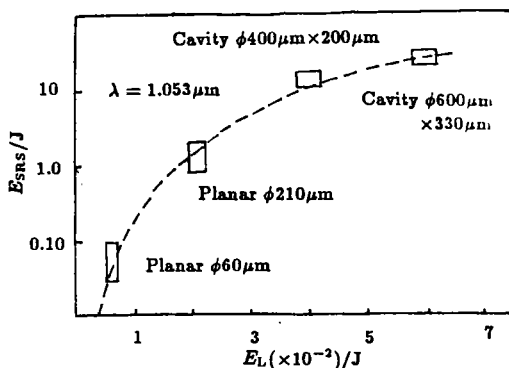


Fig.9 The dependence of SRS energy on the scale length of plasmas

## 4 Conclusion

In the nonlinear laser-plasma interaction experiments we can draw the following conclusions:

- We have obviously observed the big enhancement of SRS light by two order in cavity targets because of the cavity confinement for the plasmas. SRS and SBS are main nonlinear processes, TPD is the third nonlinear processes, the weakest are RA and IAD, they can scatter about 0.25, 0.15, 0.006 and 0.003 of laser light energy fraction, respectively.
- There is a linear correlation between the SRS light energy and hot electron energy, it indicates that hot electrons of cavity target are mainly generated by SRS.
- SRS is a sensitive function of laser parameters, target size, structure.
- Shorter wavelength laser can be used to suppress SRS and hot electrons because of increasing electron-ion collision.
- Hot electrons mostly travel along the direction of laser beam. Hard X-rays are generated at gold wall of cavity target.

## References

- Qi Lanying, Li Sanwei, Zheng Zhijian *et al.* High Power Laser and Particle Beams(in Chinese), 1993; 5(3):415
- Mei Qiyong, Zhao Xuwei, Jiang Xiaohua *et al.* High Power Laser and Particle Beams(in Chinese), 1994; 6(1):12
- Qi Lanying, Yang Xiangdong, Yi Rongqing *et al.* High Power Laser and Particle Beams(in Chinese), 1993; 5(2):309
- Tarvin J A, Bush Gare E, Gable E F *et al.* Laser and Particle Beams(USA), 1989; 4(3,4):461
- Li Sanwei, Qi Lanying, Yang Xiangdong *et al.* High Power Laser and Particle Beams(in Chinese), 1994; 6(3):400
- Turner R E. Superthermal electron production at short laser wavelengths(USA), UCRL-50021-1984,1985:5
- Turner R E. Exploding foil experiments (USA), UCRL-50021-1986,1987:4
- Rubenchik A(USSR), Witkowski S(Germany). Physics of Laser Plasma, 1991:206,363
- Rousseaux C, Amiranoff F, Labaune C *et al.* Phys Fluids(USA),1992; B4(8):2589